Published for SISSA by Springer

Received: *May 9, 2012*
Revised: *July 30, 2012*
Accepted: *August 8, 2012*
Published: *August 24, 2012*

QCD thermodynamics with continuum extrapolated Wilson fermions I

Szabolcs Borsányi,[a] **Stephan Dürr,**[a,b] **Zoltán Fodor,**[a,b,c] **Christian Hoelbling,**[a] **Sándor D. Katz,**[c] **Stefan Krieg,**[a,b] **Dániel Nógrádi**[c] **Kálmán K. Szabó,**[a] **Bálint C. Tóth**[a] **and Norbert Trombitás**[c]

[a] *University of Wuppertal, Department of Physics, Wuppertal D-42097, Germany*
[b] *Jülich Supercomputing Center, Forschungszentrum Jülich, Jülich D-52425, Germany*
[c] *Eötvös University, Institute for Theoretical Physics, Budapest 1117, Hungary*

E-mail: borsanyi@uni-wuppertal.de, durr@itp.unibe.ch, fodor@bodri.elte.hu, hch@physik.uni-wuppertal.de, katz@bodri.elte.hu, s.krieg@fz-juelich.de, nogradi@bodri.elte.hu, szaboka@general.elte.hu, tothbalint@szofi.elte.hu, trombitas@bodri.elte.hu

Abstract: QCD thermodynamics is considered using Wilson fermions in the fixed scale approach. The temperature dependence of the renormalized chiral condensate, quark number susceptibility and Polyakov loop is measured at four lattice spacings allowing for a controlled continuum limit. The light quark masses are fixed to heavier than physical values in this first study. Finite volume effects are ensured to be negligible by using approriately large box sizes. The final continuum results are compared with staggered fermion simulations performed in the fixed N_t approach. The same continuum renormalization conditions are used in both approaches and the final results agree perfectly.

Keywords: Lattice QCD, Lattice Quantum Field Theory

ArXiv ePrint: 1205.0440

doi:10.1007/JHEP08(2012)126

JHEP08(2012)126

Contents

JHEP08(2012)126

1 Introduction

As the early universe evolved a transition occured at temperatures $T \approx 150$–$200\,\mathrm{MeV}$, which is related to the spontaneous breaking of chiral symmetry in QCD. The nature of the QCD transition [1] affects our understanding of the history of the universe; see e.g. [2].

Extensive experimental work is currently being done with heavy ion collisions to study the QCD transition, most recently at the Relativistic Heavy Ion Collider, RHIC and at the Large Hadron Collider, LHC. Both for the cosmological transition and for RHIC/LHC, the net baryon densities are quite small, thus the baryonic chemical potentials μ are much less than the typical hadron masses, μ is below $50\,\mathrm{MeV}$ at RHIC, even smaller at LHC and negligible in the early universe. Thus, a calculation at $\mu = 0$ is directly applicable to the cosmological transition and most probably also determines the nature and absolute temperature of the transition at RHIC/LHC. Therefore, we carry out our analysis at $\mu = 0$. Given the far-reaching implications, it is desirable to perform this calculations in a framework that is conceptually clean. For a pedagogical review on the QCD transition at $\mu = 0$ and $\mu > 0$ see e.g. [3] and for the first continuum result at $\mu > 0$ — namely, for the curvature on the chemical potential vs. temperature plane, see [4].

When we analyze the absolute scale or any other question related to the $T > 0$ QCD transition for the physically relevant case two ingredients are quite important.

First of all, one should use physical quark masses. The nature of the transition strongly depends on the quark mass. Lattice studies and effective models showed that in the three flavor theory for small or large quark masses the transition is a first order phase transition, whereas for intermediate quark masses it is an analytic crossover. Since the nature of the transition influences the absolute scale T_c of the transition — its value, mass dependence, uniqueness etc. — the use of physical quark masses is essential for the determination of T_c, too. The absolute scale then goes into all observables. Whereas it is relatively easy to reach the physical value of the strange quark mass m_s in present day lattice simulations, it is much more difficult to work with physical up and down quark masses m_{ud}, because they are much smaller: $m_s/m_{ud} \approx 28$. In calculations with m_s/m_{ud} smaller than 28 the strange quark mass is usually tuned to its approximate physical value, whereas the average up and down quark masses are larger than the physical value.

Secondly, the nature and other characteristics of the $T > 0$ QCD transition are known to suffer from discretization errors [5, 6]. Let us mention one example which underlines the importance of removing these discretization effects by performing a controlled continuum extrapolation. The three flavor theory with a large, $a \approx 0.3\,\mathrm{fm}$ lattice spacing and standard staggered action predicts a critical pseudoscalar mass of about 300 MeV [7]. This point separates the first order and cross-over regions. If we took another discretization, with another discretization error, the critical pseudoscalar mass turns out to be much smaller, well below the physical pion mass of 135 MeV. The only way to determine the physical features of the transition is to carry out a careful continuum limit analysis. It can be safely done only in the so-called scaling regime. This regime is reached when the lattice spacing a is sufficiently small, smaller than some $a_{\max}$. Dimensionless combinations of observables approach their continuum limit value (within their error bars) in the scaling regime with a correction term $c \cdot a^n$. Here c, n and $a_{\max}$ depend on the action and on the dimensionless combination. The values of c and $a_{\max}$ are typically unknown, whereas the form of the action and the observables provide the value for n, usually without performing any simulations. To carry out a controlled continuum extrapolation at least three lattice spacings in the scaling regime are needed. Two points will always lie on a two parameter $c \cdot a^n$ curve, independently whether the lattice spacings are smaller than $a_{\max}$ or not; the third point indicates if one reached the scaling regime.

It is numerically very demanding to fulfill both conditions. There are only a few cases, for which this has been achieved. Within the staggered formalism there are full results such as the nature of the transition [1], the transition temperature [8–10], equation of state [9] and fluctuations [11].

At $\mu > 0$ lattice computations are more costly, see e.g. [12]. However the curvature of the phase line separating the hadronic and quark-gluon phases is already determined in the continuum limit [4]. Results for the possible critical point only simulations on coarse lattices are available; see e.g. [13].

It is important to note that fulfilling the second condition without fulfilling the first one still leads to universal results. In other words continuum extrapolated results with non-physical quark masses are universal. Independently of the action, simulation algorithm, scale setting procedure, they provide the same answer once the quark mass is fixed

JHEP08(2012)126

which is a non-trivial issue, but can be done e.g. by fixing the pion to Omega and kaon to Omega mass ratios: M_π/M_Ω and M_K/M_Ω. These results are not the same as they are for physical quark masses, but they are well defined and unique. Contrary to this universality, fulfilling the first condition (physical quark mass) but not the second one (continuum extrapolation) leads to non-universal, non-physical results. These results still have unknown discretization errors.

Once the available computational resources are not enough to fulfill both conditions it is more advisable to carry out calculations with non-physical quark masses but perform the continuum limit extrapolation. As we have seen such results are universal and can be cross-checked with other results obtained by other fermion formalisms, actions etc. For some recent Wilson thermodynamics results see [14–20].

In this paper we determine the temperature dependencies of a couple of observables (chiral condensate, strange susceptibility, Polyakov loop) in 2+1 flavor QCD. We use Wilson fermions with six steps of stout smearing and tree level clover improvement in the quark sector and a tree level improved action in the gauge sector; for the details of the action see [21]. Our pion is non-physical, its mass is about 545 MeV, see later for a detailed discussion for the mass.

The structure of the paper can be summarized as follows. After this brief introductory section 1 a discussion on the advantages and disadvantages of Wilson thermodynamics is presented in section 2. The main features of the action and run parameters are listed in section 3. Our choice of renormalization procedures for the various measured quantities are summarized in section 4. The results are given in section 5. In section 6 we summarize and provide an outlook.

2 Choice of the fermion formalism

This paper presents the first of a series, which deals with lattice QCD thermodynamics using Wilson fermions. The final goal is to describe several bulk observables as a function of the temperature all the way to the continuum limit with physical quark masses or in other words by approaching pion masses of 135 MeV and kaon masses of 495 MeV. While the framework has the advantage of the sound conceptual status of the Wilson fermion formulation (a), and we are already able to reach the continuum limit (b), the present work suffers from the large computational cost (c) and is therefore confined to larger than physical pion masses (d). Let us discuss these aspects in some detail.

ad a. The vast majority of the large scale lattice QCD thermodynamics projects has been carried out with staggered fermions. Staggered fermions are the cheapest formulation of lattice QCD and working with them turned out to be quite successful and provided many interesting results both at $T = 0$ and $T > 0$. In their original form they describe four degenerate fermions — tastes — and one has to take the square root or the fourth root of the fermion determinant to describe two fermions or one fermion, respectively. This procedure is somewhat unattractive and there has been an ongoing debate in the literature whether it leads to the proper universality class. Wilson fermions do not raise

JHEP08(2012)126

such theoretical questions. Furthermore, staggered fermions suffer from the so-called taste symmetry violation. It means that instead of the physical pseudo-Goldston bosons there is a tower of pseudoscalars whose masses are typically well beyond the physical pion or kaon masses. The physical spectrum is expected to be restored only in the continuum limit. In the last five years some of the authors of the present paper have carried out a large scale staggered thermodynamics program, nevertheless it is desirable to cross check those results by repeating the analyses with Wilson fermions. Its theoretical cleanness is the most important reason to perform a systematic study with Wilson fermions.

ad b. As we discussed earlier lattice results are unambiguous only in the continuum limit. To this end we carry out our analysis at four lattice spacings. As we will see the results scale quite nicely and the continuum behavior can be extracted. The results are in good agreement with the results obtained with another fermion discretization, stout smeared staggered fermions. There is, however, one important conceptual difference between Wilson and staggered thermodynamics. In the staggered case the standard procedure is to take a given temporal extent N_t to control the lattice spacing and use various gauge couplings, light and strange quark masses β, m_{ud} and m_s to change the temperature. The set of parameters β, m_{ud} and m_s, for which the physical content is the same (e.g. the ratio of the kaon decay constant and the pseudoscalar masses: f_K/M_π and f_K/M_K) are called lines of constant physics (LCP). The fixed scale approach of Wilson thermodynamics [14] is in some sense the opposite. One takes a given β to fix the lattice spacing and uses several N_t values to scan the temperature. The reason for this choice is the difficulty with the additive mass renormalization within the Wilson formalism. This additive term makes it particularly difficult to give the LCPs with good numerical precision. The fixed scale approach ensures by definition that the physical content remains the same (same bare parameters) even if we change the temperature.

ad c. Wilson fermions are usually more expensive than staggered fermions. There are at least two reasons for that. First of all the basic calculational step, fermion matrix $\times$ spinor multiplication, has four times as many floating point operations for Wilson fermions as for staggered fermions. Secondly, the computational costs for the inversion of the fermion matrix strongly depends on its condition number. The condition number for the fermion matrix has a strict bound given by the quark mass for the staggered case, whereas for the same quark mass with Wilson fermions the condition number can be much larger. It depends not only on the mass but also on the gauge configuration and thus fluctuates more.

ad d. Today, the large computational costs allow to study only systems with larger than physical pion masses; larger mass means smaller condition number, thus smaller computational costs. As we discussed earlier it is more reasonable to carry out a study with larger than physical mass and extrapolate to the continuum limit than use smaller or even physical quark masses at one or two lattice spacings only. The reason for that is simple: continuum extrapolated results can be compared with those of other groups and/or lattice actions. A non-continuum result has still an unknown uncertainty due to cutoff effects. As we mentioned we compare our findings in this paper using Wilson fermions with our earlier results using staggered fermions. A nice agreement is found.

JHEP08(2012)126

3 Simulation points and techniques

In this section the details of the Wilson simulations are outlined. We also performed staggered simulations in order to compare the continuum results of the two formulations. The techniques of the staggered simulations follow [8, 9] and are shortly summarized too.

3.1 Action

The gauge action used for the calculations was the Symanzik tree level improved gauge action [22, 23]

$$S_G^{\mathrm{Sym}} = \beta \left[\frac{c_0}{3} \sum_{\mathrm{plaq}} \mathrm{Re}\,\mathrm{Tr}\,(1 - U_{\mathrm{plaq}}) + \frac{c_1}{3} \sum_{\mathrm{rect}} \mathrm{Re}\,\mathrm{Tr}\,(1 - U_{\mathrm{rect}}) \right], \tag{3.1}$$

with the parameters $c_0 = 5/3$ and $c_1 = -1/12$. The action for the femionic sector was the clover improved [24] Wilson action

$$S_F^{\mathrm{SW}} = S_F^{\mathrm{W}} - \frac{c_{\mathrm{SW}}}{4} \sum_x \sum_{\mu,\nu} \overline{\psi}_x \, \sigma_{\mu\nu} F_{\mu\nu,x} \, \psi_x \,, \tag{3.2}$$

where S_F^{W} is the Wilson fermion action. Six steps of stout smearing [25] with smearing parameter $\varrho = 0.11$ were used. The clover coefficient was set to its tree level value, $c_{\mathrm{SW}} = 1.0$, which, for this type of smeared fermions, essentially leads to an $\mathcal{O}(a)$ improved action [26] with improved chiral properties [27].

3.2 Simulation algorithm

The bare masses of the u and d quarks were taken to be degenerate, therefore the configurations were generated using an $N_f = 2+1$ flavor algorithm. The light quarks were implemented via the Hybrid Monte Carlo (HMC) algorithm [28], whereas the strange quark was implemented using the Rational Hybrid Monte Carlo (RHMC) algorithm [29]. In order to speed up the molecular dynamics calculations, the Sexton-Weingarten multiple time-scale integration scheme [30] combined with the Omelyan integrator [31] was employed. When all four extents of the lattice were even, the usage of even-odd preconditioning [32] gave an additional speed up factor of 2. For further details on the algorithm see [21].

3.3 Simulation points

The calculations were performed at four different gauge couplings, $\beta = 3.30$, 3.57, 3.70 and 3.85. Only dimensionless ratios are measured and every dimensionful quantity is made dimensionless by appropriate powers of m_Ω or m_π. The lattice spacing is also set by the physical value $m_\Omega = 1672\,MeV$ and the four gauge couplings correspond to $a = 0.139(1)$, $0.093(1)$, $0.070(1)$ and $0.057(1)$ fm, respectively. At all four gauge couplings the bare masses are tuned such that $m_\pi/m_\Omega = 0.326(4)$ and $m_K/m_\Omega = 0.366(4)$ are constant, which means that $m_\pi \approx 545\,\mathrm{MeV}$ and $m_K \approx 614\,\mathrm{MeV}$. We tried to tune the m_s/m_{ud} ratio to the same value $m_s/m_{ud} = 1.5$ as used in the staggered reference runs. We achieved this within 2% accuracy: the ratio $(2m_K^2 - m_\pi^2)/m_\pi^2$ which in leading order chiral perturbation

JHEP08(2012)126

β	am_{ud}	am_s	N_s	N_t
3.30	-0.0985	-0.0710	32	4–16, 32
3.57	-0.0260	-0.0115	32	4–16, 64
3.70	-0.0111	0.0	48	8–28, 48
3.85	-0.00336	0.0050	64	12–28, 64

Table 1. Simulation parameters. The N_t values used for the finite temperature runs and the values used for the zero temperature runs are separated by a comma.

theory equals m_s/m_{ud} is 1.530(7) for all four gauge couplings. All four values of m_s are such that if m_{ud} is lowered to the physical point m_K also becomes the physical kaon mass. The bare quark masses, spatial and temporal lattice extents are shown in table 1 while the measured masses are shown in table 2. In all four cases $m_\pi L_s \gtrsim 8$. At each finite temperature point around 1000 equilibrated trajectories were generated while around 500 at zero temperature points.

3.4 Staggered simulations

The goal of the staggered simulations detailed below was to provide a basis of comparison for the Wilson data. We used the staggered action with two steps of stout smearings ($\varrho = 0.15$) as in most our thermodynamics studies e.g. [8]. The line of constant physics used there was extended to the fine lattices in [9, 33, 34]. We used the bare strange masses for each given beta as were determined there. The light quark mass was simply set to 2/3 of the strange mass to achieve the desired pion/kaon mass ratio. The lattice spacing in these staggered thermodynamics papers was set through the kaon decay constant. For each used gauge coupling we determined the scale directly with zero temperature runs at the light/strange mass ratio 2/3. Using the most precise scale setting observable we had access to, the w_0 scale [35], we checked that our original scale function was still correct. We proceeded to compute the mass ratios $m_\pi/m_\Omega \simeq 0.32$ and $M_K/m_\Omega \simeq 0.36$ that turned out to agree with the Wilson values at the level of 3% in both cases.

For the renormalization we used dedicated zero temperature runs with parameters precisely matching those in the finite temperature simulations. We determined the vacuum condensate $\langle\bar{\psi}\psi\rangle_0$ and the static potential $V(r)$, which we needed for obtaining the multiplicative renormalization of the Polyakov loop: $Z = \exp(V(x)/2)$. The obtained finite renormalized Polyakov loop is then further transformed to our scheme (see section 4.4) by a finite renormalization factor. One can select any physical scale x to remove all divergences. Since w_0 is our most accurately known scale, we used $x = \sqrt{8}w_0$, which is approximately $0.5\,fm$. We found that in the continuum, at this mass ratio we have $m_\Omega w_0 = 1.466(15)$.

Our finite temperature staggered simulations were performed on $18^3\times6$, $24^3\times8$, $32^3\times10$ and $36^3\times12$ lattices. After performing the necessary steps of renormalization a continuum extrapolation was carried out. For this extrapolation we used a cubic spline interpolation (using roughly every second temperatures as node points). Then for every temperature we

JHEP08(2012)126

β	m_π/m_Ω	m_K/m_Ω	m_s/m_{ud}	am_{PCAC}	am_Ω	$a\,[fm]$	Z_A
3.30	0.332(3)	0.373(3)	1.529(2)	0.0428(2)	1.16(1)	0.139(1)	0.892(7)
3.57	0.319(6)	0.359(4)	1.531(2)	0.02649(4)	0.777(9)	0.093(1)	0.951(2)
3.70	0.326(5)	0.369(5)	1.531(3)	0.01994(4)	0.586(8)	0.070(1)	0.966(2)
3.85	0.314(7)	0.358(6)	1.528(4)	0.01559(2)	0.480(8)	0.057(1)	0.976(5)

Table 2. Spectroscopy and Z_A renormalization constant results from zero temperature simulations. The m_s/m_{ud} column refers to $(2m_K^2 - m_\pi^2)/m_\pi^2$. The lattice spacings are set by $m_\Omega = 1672\,\mathrm{MeV}$.

evaluated several possible extrapolations (linear in a^2). The choices included using all four lattice spacings or just three of them, and also making the extrapolation for the reciprocal observable. The width of the weighted histogram of the continuum extrapolations define a systematic error, which we added to the statistical error in quadrature. The final continuum extrapolation includes an additional overall percent-level error in the temperature axis.

4 Renormalization

The bare chiral condensate is divergent in the continuum limit and both additive (power-like) and multiplicative (logarithmic) divergences need to be removed. The resulting finite chiral condensate in the continuum limit can be compared with results obtained using other regularizations for instance the staggered formulation since finite continuum quantities should not depend on the regulator.

The additive and multiplicative renormalizations are treated separately in the following two subsections. We follow [36] which is based on [37]. The measurement of the finite renormalization constant Z_A is outlined in subsection 4.3. The Polyakov loop also needs to be renormalized and our scheme is defined below in subsection 4.4.

4.1 Additive renormalization of the condensate

On dimensional grounds the bare chiral condensate contains additive divergences of the type

$$\frac{\langle\bar{\psi}_0\psi_0\rangle}{N_f} = c_0 + c_1(m_0 - m_c) + c_2(m_0 - m_c)^2 + \dots \tag{4.1}$$

where m_0 is the dimensionful bare mass, m_c is its critical value and c_0 is cubically, c_1 is quadratically and c_2 is linearly divergent. The coefficients c_i do not depend on the temperature hence they cancel in the quantity

$$\frac{\Delta_{\bar{\psi}\psi}(T)}{N_f} = \frac{\langle\bar{\psi}_0\psi_0\rangle(T) - \langle\bar{\psi}_0\psi_0\rangle(T=0)}{N_f} \tag{4.2}$$

just like in the staggered case. The cancellation is of order $O(a^{-3})$.

However the $O(a^{-3})$ term in (4.1) can be explicitly removed and the following quantity is free of cubic divergences [36],

$$\frac{\langle\bar{\psi}_0\psi_0\rangle}{N_f} - c_0 = 2m_{PCAC}Z_A \int d^4x \langle P_0(x)P_0(0)\rangle + \cdots\,, \tag{4.3}$$

JHEP08(2012)126

but of course quadratically and linearly divergent pieces are still present. Here $P_0(x)$ is the bare pseudo-scalar condensate, m_{PCAC} is the PCAC mass and $Z_A(g_0)$ is a finite renormalization constant [36]. Our conventions for the definition of $P_0(x)$ and $\langle\bar{\psi}_0\psi_0\rangle$ are the same as in [36]. Hence for the subtracted condensate we have,

$$\frac{\Delta_{\bar{\psi}\psi}(T)}{N_f} = 2m_{PCAC}Z_A\Delta_{PP}(T) + \cdots , \tag{4.4}$$

where the short hand notation

$$\Delta_{PP}(T) = \int d^4x\langle P_0(x)P_0(0)\rangle(T) - \int d^4x\langle P_0(x)P_0(0)\rangle(T=0) \tag{4.5}$$

was introduced. In (4.5) the cancellation between the finite and zero temperature terms is only $O(a^{-2})$ however all additive divergences are still removed.

4.2 Multiplicative renormalization of the condensate

Multiplicative logarithmic divergences are still present in both (4.2) and (4.4). Multiplying both expressions by first Z_P and then by a renormalized mass $m_R = m_{PCAC}Z_A/Z_P$ leads to a renormalization group invariant quantity $m_R\langle\bar{\psi}\psi\rangle_R$. Hence using (4.2), (4.4) and (4.5) we arrive at the expressions,

$$m_R\langle\bar{\psi}\psi\rangle_R(T) = 2N_f m_{PCAC}^2 Z_A^2\Delta_{PP}(T) \tag{4.6}$$

$$m_R\langle\bar{\psi}\psi\rangle_R(T) = m_{PCAC}Z_A\Delta_{\bar{\psi}\psi}(T) + \cdots , \tag{4.7}$$

where the former may be taken as the definition of $\langle\bar{\psi}\psi\rangle_R(T)$ and the latter agrees with it in the continuum limit. Both are of course also finite. The finite cut-off corrections for (4.6) is $O(a^2)$ at tree level provided the action is $O(a)$-improved, because the tree level improvement factors for m_R and $\langle\bar{\psi}\psi\rangle_R$ cancel in the product. The full non-perturbative improvement of m_R and $\langle\bar{\psi}\psi\rangle_R$ we expect to be close to tree level improvement because our smeared action with tree level improvement coefficient $c_{\rm SW} = 1.0$ is very close to being non-perturbatively $O(a)$-improved [26, 27]. The quantities $\Delta_{\bar{\psi}\psi}(T)$ and $\Delta_{PP}(T)$ on the right hand sides are easy to measure on the lattice and knowing m_{PCAC} and Z_A from zero temperature simulations allows one to define the finite and renormalization group invariant continuum quantity $m_R\langle\bar{\psi}\psi\rangle_R(T)$ in two different ways. In the continuum limit the two definitions should agree within errors.

On the other hand, using the first expression in (4.7) to solve for $m_{PCAC}Z_A$ and substituting it into the second expression leads to,

$$m_R\langle\bar{\psi}\psi\rangle_R(T) = \frac{\Delta^2_{\bar{\psi}\psi}(T)}{2N_f\Delta_{PP}(T)} + \cdots , \tag{4.8}$$

which can directly be measured from the bare quantities $\Delta_{\bar{\psi}\psi}(T)$ and $\Delta_{PP}(T)$ without any need for measuring m_{PCAC} or the Z_A renormalization factor. In [38] the above ratio was used to define the chiral condensate, in the present study we will use (4.6) because we have found that this definition of the renormalized condensate scales best among the three possible choices (4.6), (4.7) and (4.8).

JHEP08(2012)126

4.3 Computation of Z_A

We compute the renormalization constant of the local axial vector current Z_A along the lines presented in [39, 40]. We generated independent sets of $N_f = 3$ ensembles at four quark masses in the range $m_s/3 < m_q < m_s$ and approximately equal physical volume $V \simeq (2\ \mathrm{fm})^4$ at every β.

In a first step, we compute the local vector current renormalization constant Z_V from the ratio

$$\xi(t) = \frac{\langle P_0(N_t/2)V_0(t)P_0(0)\rangle}{\langle P_0(N_t/2)P_0(0)\rangle} \tag{4.9}$$

where

$$P_0(t) = \int d^3x P_0(t,\vec{x})\ , \qquad V_0(t) = \int d^3x\,(\bar{\psi}_1\gamma_0\psi_1)(t,\vec{x})\ , \tag{4.10}$$

are the zero 3-momentum projected bare pseudo-scalar and vector densities. With tree level improvement one has [41, 42]

$$Z_V(\beta,m)(1+am) = (\xi(t_1)-\xi(t_2))^{-1} \quad \text{for} \quad 0 < t_1 < N_t/2 < t_2 < N_t \tag{4.11}$$

We obtain Z_A by using the standard RI-MOM procedure [43] with the improvement technique of [44] to determine the ratio

$$\frac{Z_A(\beta,m)}{Z_V(\beta,m)} = \frac{\Gamma_V(p)}{\Gamma_A(p)} \tag{4.12}$$

from the off-shell amputated Greens functions $\Gamma_\Gamma(p)$. The dependence of the ratio (4.12) on the external quark momenta p is very mild and enters into our estimate of the systematic error. We linearly extrapolate the resulting $Z_A(\beta,m)$ to $m = 0$ to obtain the renormalization constant $Z_A(\beta)$, see table 2.

4.4 Polyakov loop

The real part of the bare Polyakov loop also needs to be renormalized [8] in order to have a quantity with a finite continuum limit. Since there is an additive divergence in the free energy, a convenient choice of renormalization prescription is demanding a fixed value L_* for the renormalized Polyakov loop at a fixed but arbitrary temperature $T_* > T_c$. Then the renormalized Polyakov loop L_R is given by

$$L_R(T) = \left(\frac{L_*}{L_0(T_*)}\right)^{\frac{T_*}{T}} L_0(T) \tag{4.13}$$

in terms of the bare Polyakov loop $L_0(T)$. We choose $T_* = 0.143 m_\Omega$ and $L_* = 1.2$. Other choices would simply correspond to other renormalization schemes.

We imposed the same renormalization condition on the central value of our continuum extrapolated staggered data so they can be meaningfully compared.

JHEP08(2012)126

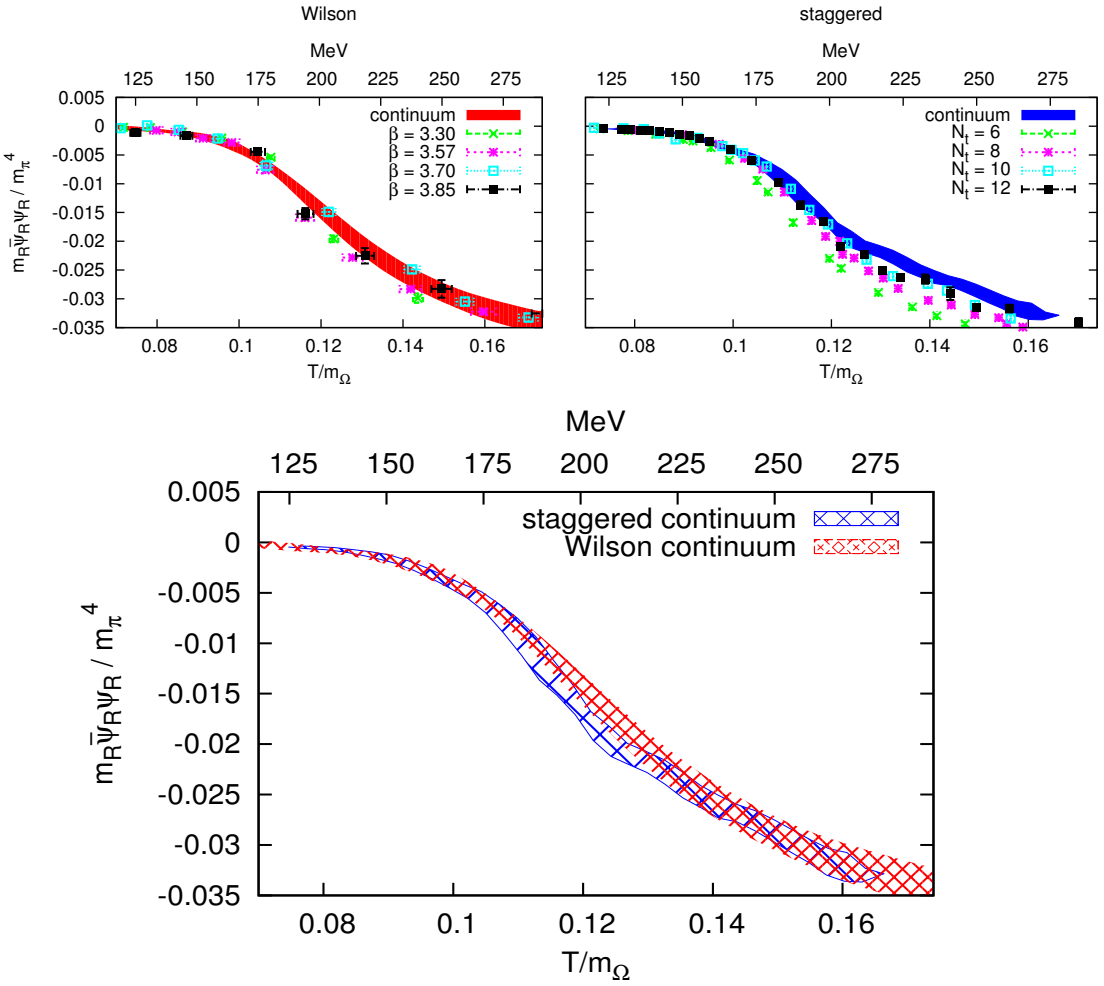

Figure 1. Renormalized chiral condensate. The top left panel shows the Wilson results using the definition (4.6) at the four lattice spacings corresponding to four β values. The continuum extrapolated result is also shown by the solid band. The top right panel shows the staggered results in the fixed-N_t approach also together with the continuum extrapolated result. The bottom panel compares the two continuum results.

5 Results

We have measured three quantities at each lattice spacing. The renormalized chiral condensate is sensitive to the remnant of the chiral transition whereas the renormalized Polyakov loop and the strange quark number susceptibility are sensitive to the remnant of the confinement-deconfinement transition.

Each quantity is renormalized properly so that in the continuum limit finite and regularization scheme independent values are obtained. The Wilson continuum extrapolation is based on a cubic spline interpolation to temperatures not reachable by the discrete range of N_t and extrapolation $a \to 0$. We perform global fits to all our data points including lattice spacing dependence in the fit parameters as follows. Spline node points are randomly distributed along the temperature axis. The parameters of our fit are the values of the ob-

JHEP08(2012)126

N_t	8	10	12	14	16	18	20	22	24	26
SB	1.522	1.265	1.161	1.110	1.081	1.062	1.049	1.040	1.034	1.028

Table 3. The tree level improvement factors of the strange quark number susceptibility for Wilson fermions. The values shown are the free, infinite volume, massless Stefan-Boltzmann limits at given N_t. For $\beta = 3.30$ and 3.57 only $N_t \geq 8$, for $\beta = 3.70$ only $N_t \geq 12$ and for $\beta = 3.85$ only $N_t \geq 14$ is used.

servable at the node points together with their lattice spacing dependence, i.e. $o_{1i} + c(a)o_{2i}$ for the i^{th} node point. For the leading correction $c(a)$ we used two choices, $c(a) = a^2$ and $c(a) = \alpha a$. We had 4-6 nodepoints with 1000 different random node point sets each, resulting in $2 \cdot 3 \cdot 1000 = 6000$ fits alltogether. The results of the fits are weighted with the fit qualities. For each temperature the median of these fits is used as our final result and the systematic error comes from the central 68% of the distribution and the statistical error from a jackknife analysis. The simulations were performed at 4 lattice spacings but not every observable is measured in the full temperature range. For the temperature range where our final results are presented we had at least 3 lattice spacings available in other words at least 3 lattice spacings are used for the continuum extrapolation. The obtained continuum results can then be compared with results from other regularizations such as the staggered formulation.

Figure 1 shows the renormalized chiral condensate. The left panel contains the Wilson simulation results at four lattice spacings together with the continuum extrapolated result. The right panel shows the chiral condensate result for the staggered calculation at 4 fixed N_t values 6, 8, 10 and 12 corresponding to four lattice spacings. Cubic spline is used to interpolate at fixed N_t and these are then extrapolated to the continuum. The middle panel shows the two continuum extrapolated results. They are in perfect agreement.

In an earlier exploratory work we used the definition (4.8) for the renormalized chiral condensate resulting in much larger cut-off effects [38]. The reason for using (4.6) this time is exactly because the cut-off effects are smaller as is visible from figure 1 compared to figure 1 in [38].

The strange quark number susceptibility $\chi_s = T/V\, \partial^2 \log(Z)/\partial \mu_s^2$ is a sum of two contributions, the connected and disconnected terms. The disconnected part is a very noisy quantity (as usual) and a large number of random vectors, 1200, were needed in order to evaluate it precisely. It is advantageous to generate the random vectors in the 12 diagonal spin-color blocks separately [15]. Cut-off effects may be reduced by tree level improvement. The measured susceptibility is divided by its infinite volume, massless Stefan-Boltzmann limit at the given finite N_t temporal extent. The continuum limit is unchanged by this improvement since the Stefan-Boltzmann limits are 1 for $N_t \to \infty$; see table 3.

The results for the four lattice spacings are shown on figure 2 together with the staggered results. What is plotted in both cases is the aforementioned tree level improved quark number susceptibility.

The number of data points is less for the quark number susceptibility than for the chiral condensate because for the condensate odd N_t values are used as well. In such a

JHEP08(2012)126

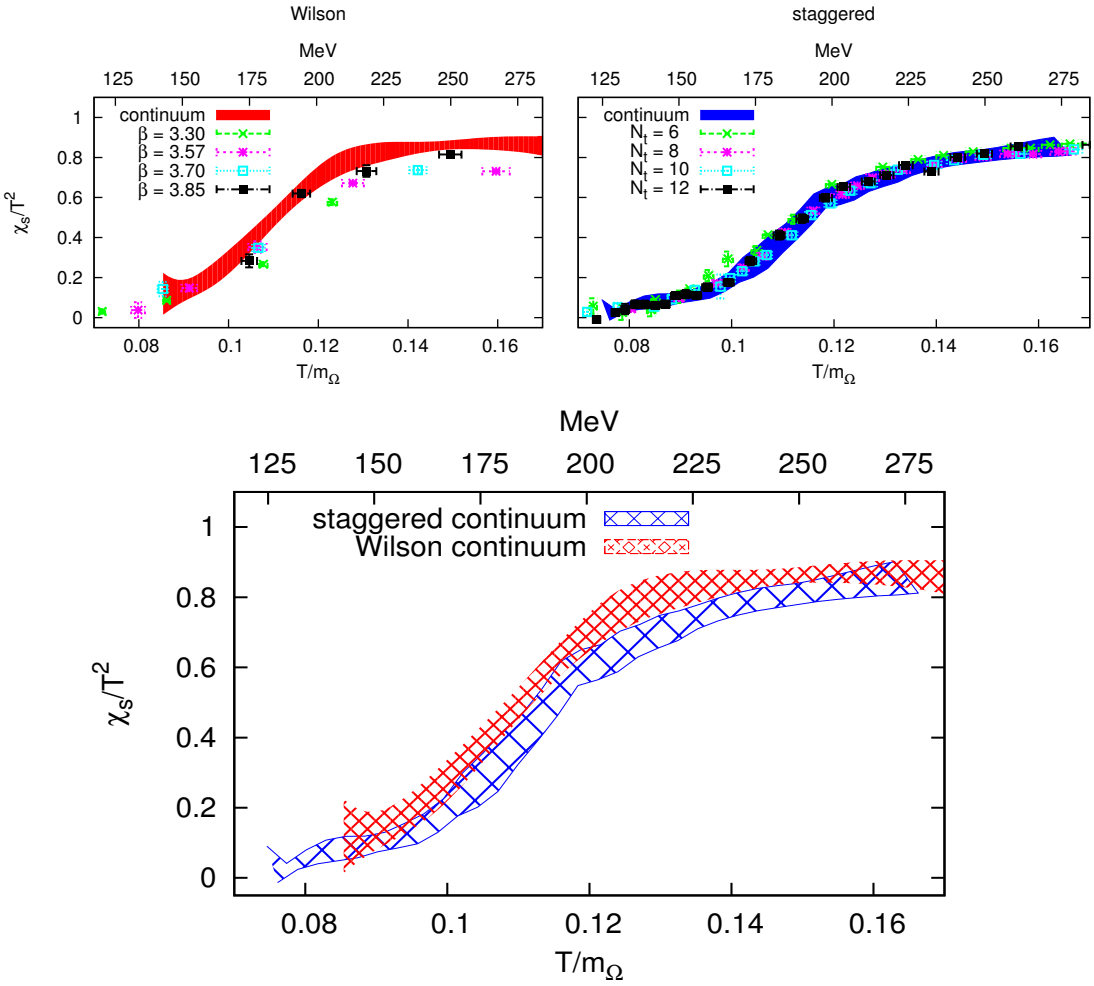

Figure 2. Strange quark number susceptibility. The top left panel shows the Wilson results at the four lattice spacings corresponding to four β values. The continuum extrapolated result is also shown by the solid band. The top right panel shows the staggered results in the fixed-N_t approach also together with the continuum extrapolated result. The bottom panel compares the two continuum results.

setup even-odd preconditioning can not be used resulting in a much slower simulation and measurement. The large number of random vectors needed also forced us to also skip some even N_t values in some cases only having those that are divisible by 4.

Discretization errors are comparable to the chiral condensate. The results are shown on figure 2 again with the Wilson results on the left, staggered results on the right and the comparison of the two continuum results in the middle. Again the agreement between the two continuum extrapolated results is perfect.

The third quantity we measured is the renormalized Polyakov loop which is sensitive to the confinement-deconfinement transition similarly to the quark number susceptibility. The results are shown on figure 3 in the same format as before; Wilson results on the left, staggered results on the right with the comparison of the two continuum extrapolated curves

JHEP08(2012)126

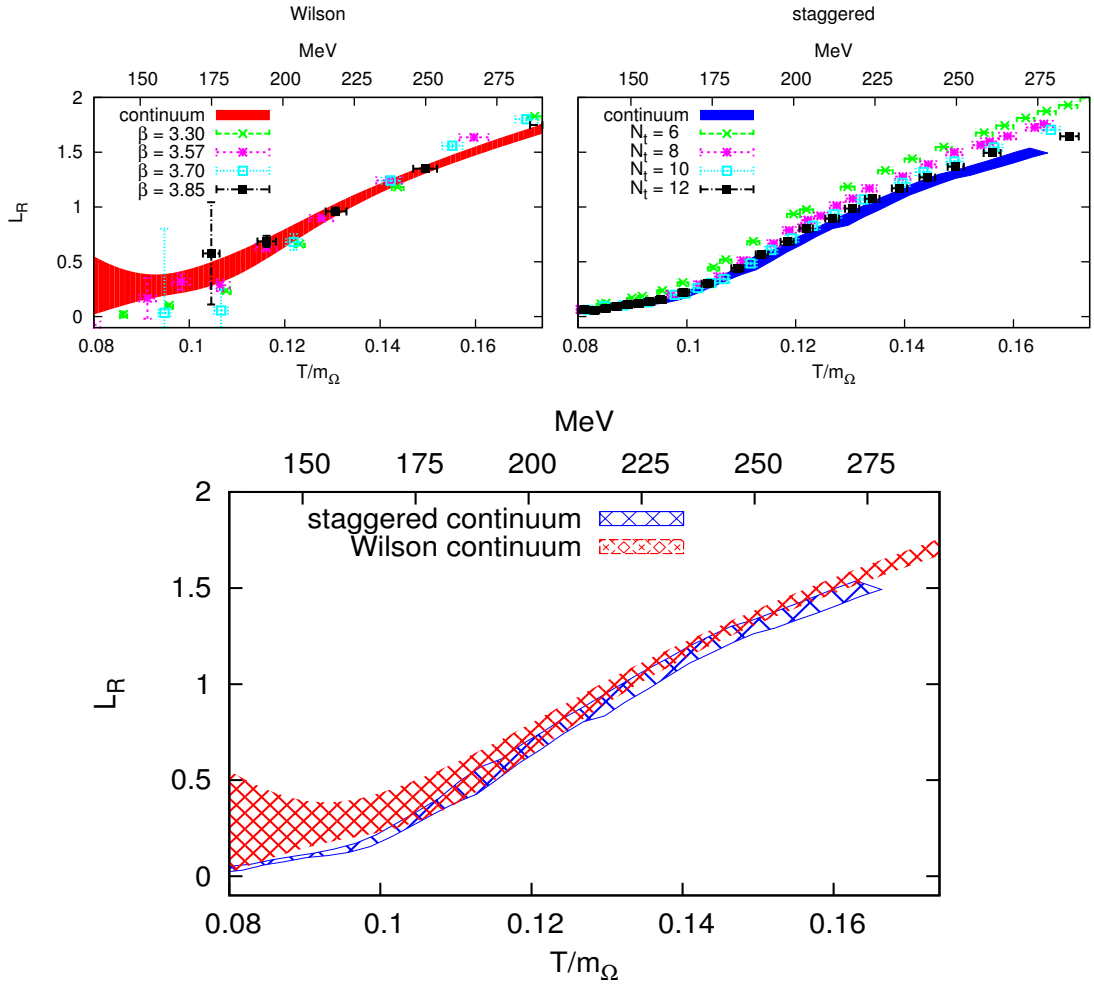

Figure 3. Renormalized Polyakov loop. The top left panel shows the Wilson results at the four lattice spacings corresponding to four β values. The continuum extrapolated result is also shown by the solid band. The top right panel shows the staggered results in the fixed-N_t approach also together with the continuum extrapolated result. The bottom panel compares the two continuum results.

in the middle. The bare Polyakov loop can be measured quite precisely but renormalization in our scheme at low temperatures causes the errors to increase because of the division and high power in equation (4.13). For higher temperatures the errors are smaller where the renormalization condition (4.13) does not introduce large uncertainties.

6 Summary and outlook

In this work finite temperature QCD was studied using Wilson discretization for $2 + 1$ flavors of dynamical fermions. The unique aspect of our work is the continuum extrapolation of all three renormalized quantities we have measured, chiral condensate, strange quark number susceptibility and Polyakov loop, which is especially difficult with Wilson fermions. The difficulty lies in the fact that the explicit chiral symmetry breaking of the Wilson formulation necessitates fine lattice spacings and consequently large lattice volumes.

JHEP08(2012)126

The continuum extrapolation has been carried out for all temperatures and by using four lattice spacings.

The motivation for our work is twofold. First, it is desirable to obtain continuum QCD results from first principles which do not contain theoretically not fully justified operations such as the fourth root trick of rooted staggered fermions. The Wilson fermion formulation is theoretically sound and is known to be in the right universality class for QCD. Second, since a large body of simulation results for both zero and finite temperatures exist with the staggered formulation it is a worthwhile task to compare some of these continuum results with the continuum Wilson results. The expectation is of course that if the staggered formulation is also in the right universality class the continuum results will agree within errors.

The Wilson formulation is more expensive than the staggered formulation hence lowering the light quark masses towards their physical value is much more difficult. In this work the pion mass has been set to 545 MeV, heavier than physical, but it is important to note that at arbitrary quark masses the continuum results are universal. Hence provided the same renormalization prescription is used for two discretizations the results should still agree in the continuum for arbitrary quark masses. We have carried out staggered simulations using the same renormalization prescription as we did for the Wilson simulations and have compared the continuum extrapolated results. Nice agreement was found for all three quantities.

In the future we plan to lower the light quark masses towards their physical value. With an unimproved fermion action this would be almost hopeless however the use of stout improvement makes the fluctuation of low lying Dirac eigenvalues much less allowing for a smaller pion mass at a given volume.

We also plan to compare the continuum extrapolated staggered and Wilson results with a formulation which combines the key advantages of the two: chiral symmetry (staggered) and theoretical soundness (Wilson). Such a lattice chiral discretization is the overlap formalism. Results at two lattice spacings are already available in the fixed-N_t approach [45]. Once completed with a third or fourth lattice spacing a continuum extrapolation will be possible allowing for the comparison of three continuum results from three discretizations of QCD.

Acknowledgments

Computations were carried out on GPU clusters [46] at the Universities of Wuppertal and Budapest as well as on supercomputers in Forschungszentrum Juelich.

This work was supported by the EU Framework Programme 7 grant (FP7/2007-2013)/ERC No 208740 and by the Deutsche Forschungsgemeinschaft grants FO 502/2 and SFB-TR 55.

References

[1] Y. Aoki, G. Endrodi, Z. Fodor, S. Katz and K. Szabo, *The order of the quantum chromodynamics transition predicted by the standard model of particle physics*, *Nature* **443** (2006) 675 [hep-lat/0611014] [INSPIRE].

JHEP08(2012)126

[2] D.J. Schwarz, *The first second of the universe*, *Annalen Phys.* **12** (2003) 220 [astro-ph/0303574] [INSPIRE].

[3] Z. Fodor and S. Katz, *The phase diagram of quantum chromodynamics*, arXiv:0908.3341 [INSPIRE].

[4] G. Endrodi, Z. Fodor, S. Katz and K. Szabo, *The QCD phase diagram at nonzero quark density*, *JHEP* **04** (2011) 001 [arXiv:1102.1356] [INSPIRE].

[5] P. de Forcrand, S. Kim and O. Philipsen, *A QCD chiral critical point at small chemical potential: is it there or not?*, PoS(LATTICE 2007)178 [arXiv:0711.0262] [INSPIRE].

[6] G. Endrodi, Z. Fodor, S. Katz and K. Szabo, *The nature of the finite temperature QCD transition as a function of the quark masses*, PoS(LATTICE 2007)182 [arXiv:0710.0998] [INSPIRE].

[7] F. Karsch, E. Laermann and C. Schmidt, *The chiral critical point in three-flavor QCD*, *Phys. Lett.* **B 520** (2001) 41 [hep-lat/0107020] [INSPIRE].

[8] Y. Aoki, Z. Fodor, S. Katz and K. Szabo, *The QCD transition temperature: results with physical masses in the continuum limit*, *Phys. Lett.* **B 643** (2006) 46 [hep-lat/0609068] [INSPIRE].

[9] Y. Aoki et al., *The QCD transition temperature: results with physical masses in the continuum limit II*, *JHEP* **06** (2009) 088 [arXiv:0903.4155] [INSPIRE].

[10] A. Bazavov et al., *The chiral and deconfinement aspects of the QCD transition*, *Phys. Rev.* **D 85** (2012) 054503 [arXiv:1111.1710] [INSPIRE].

[11] S. Borsányi et al., *Fluctuations of conserved charges at finite temperature from lattice QCD*, *JHEP* **01** (2012) 138 [arXiv:1112.4416] [INSPIRE].

[12] Z. Fodor and S. Katz, *A new method to study lattice QCD at finite temperature and chemical potential*, *Phys. Lett.* **B 534** (2002) 87 [hep-lat/0104001] [INSPIRE].

[13] Z. Fodor and S. Katz, *Critical point of QCD at finite T and μ, lattice results for physical quark masses*, *JHEP* **04** (2004) 050 [hep-lat/0402006] [INSPIRE].

[14] T. Umeda et al., *Fixed scale approach to equation of state in lattice QCD*, *Phys. Rev.* **D 79** (2009) 051501 [arXiv:0809.2842] [INSPIRE].

[15] WHOT-QCD collaboration, S. Ejiri et al., *Equation of state and heavy-quark free energy at finite temperature and density in two flavor lattice QCD with wilson quark action*, *Phys. Rev.* **D 82** (2010) 014508 [arXiv:0909.2121] [INSPIRE].

[16] WHOT-QCD collaboration, Y. Maezawa et al., *Free energies of heavy quarks in full-QCD lattice simulations with Wilson-type quark action*, *Nucl. Phys.* **A 830** (2009) 247C–250C [arXiv:0907.4203] [INSPIRE].

[17] V. Bornyakov et al., *Probing the finite temperature phase transition with $N_f = 2$ nonperturbatively improved Wilson fermions*, *Phys. Rev.* **D 82** (2010) 014504 [arXiv:0910.2392] [INSPIRE].

[18] WHOT-QCD collaboration, T. Umeda et al., *EOS in $2+1$ flavor QCD with improved Wilson quarks by the fixed-scale approach*, PoS(LATTICE 2010)218 [arXiv:1011.2548] [INSPIRE].

[19] Y. Maezawa et al., *Application of fixed scale approach to static quark free energies in quenched and $2+1$ flavor lattice QCD with improved Wilson quark action*, arXiv:1112.2756 [INSPIRE].

JHEP08(2012)126

[20] WHOT-QCD collaboration, T. Umeda et al., *Equation of state in $2+1$ flavor QCD with improved Wilson quarks by the fixed scale approach*, *Phys. Rev.* **D 85** (2012) 094508 [arXiv:1202.4719] [INSPIRE].

[21] S. Dürr et al., *Scaling study of dynamical smeared-link clover fermions*, *Phys. Rev.* **D 79** (2009) 014501 [arXiv:0802.2706] [INSPIRE].

[22] K. Symanzik, *Continuum limit and improved action in lattice theories. 1. Principles and ϕ^4 theory*, *Nucl. Phys.* **B 226** (1983) 187 [INSPIRE].

[23] M. Lüscher and P. Weisz, *On-shell improved lattice gauge theories*, *Commun. Math. Phys.* **97** (1985) 59 [*Erratum ibid.* **98** (1985) 433] [INSPIRE].

[24] B. Sheikholeslami and R. Wohlert, *Improved continuum limit lattice action for QCD with Wilson fermions*, *Nucl. Phys.* **B 259** (1985) 572 [INSPIRE].

[25] C. Morningstar and M.J. Peardon, *Analytic smearing of* SU(3) *link variables in lattice QCD*, *Phys. Rev.* **D 69** (2004) 054501 [hep-lat/0311018] [INSPIRE].

[26] R. Hoffmann, A. Hasenfratz and S. Schaefer, *Non-perturbative improvement of nHYP smeared Wilson fermions*, PoS(LATTICE 2007)104 [arXiv:0710.0471] [INSPIRE].

[27] S. Capitani, S. Dürr and C. Hölbling, *Rationale for UV-filtered clover fermions*, *JHEP* **11** (2006) 028 [hep-lat/0607006] [INSPIRE].

[28] S. Duane, A. Kennedy, B. Pendleton and D. Roweth, *Hybrid Monte Carlo*, *Phys. Lett.* **B 195** (1987) 216 [INSPIRE].

[29] M. Clark and A. Kennedy, *Accelerating dynamical fermion computations using the rational hybrid Monte Carlo (RHMC) algorithm with multiple pseudofermion fields*, *Phys. Rev. Lett.* **98** (2007) 051601 [hep-lat/0608015] [INSPIRE].

[30] J. Sexton and D. Weingarten, *Hamiltonian evolution for the hybrid Monte Carlo algorithm*, *Nucl. Phys.* **B 380** (1992) 665 [INSPIRE].

[31] T. Takaishi and P. de Forcrand, *Testing and tuning new symplectic integrators for hybrid Monte Carlo algorithm in lattice QCD*, *Phys. Rev.* **E 73** (2006) 036706 [hep-lat/0505020] [INSPIRE].

[32] T.A. DeGrand, *A conditioning technique for matrix inversion for Wilson fermions*, *Comput. Phys. Commun.* **52** (1988) 161 [INSPIRE].

[33] Wuppertal-Budapest collaboration, S. Borsányi et al., *Is there still any T_c mystery in lattice QCD? Results with physical masses in the continuum limit III*, *JHEP* **09** (2010) 073 [arXiv:1005.3508] [INSPIRE].

[34] S. Borsányi et al., *The QCD equation of state with dynamical quarks*, *JHEP* **11** (2010) 077 [arXiv:1007.2580] [INSPIRE].

[35] S. Borsányi et al., *High-precision scale setting in lattice QCD*, arXiv:1203.4469 [INSPIRE].

[36] L. Giusti, F. Rapuano, M. Talevi and A. Vladikas, *The QCD chiral condensate from the lattice*, *Nucl. Phys.* **B 538** (1999) 249 [hep-lat/9807014] [INSPIRE].

[37] M. Bochicchio, L. Maiani, G. Martinelli, G.C. Rossi and M. Testa, *Chiral symmetry on the lattice with Wilson fermions*, *Nucl. Phys.* **B 262** (1985) 331 [INSPIRE].

[38] S. Borsányi et al., *QCD thermodynamics with Wilson fermions*, PoS(LATTICE 2011)209 [arXiv:1111.3500] [INSPIRE].

[39] S. Dürr et al., *Lattice QCD at the physical point: light quark masses*, *Phys. Lett.* **B 701** (2011) 265 [arXiv:1011.2403] [INSPIRE].

JHEP08(2012)126

[40] S. Dürr et al., *Lattice QCD at the physical point: simulation and analysis details*, *JHEP* **08** (2011) 148 [arXiv:1011.2711] [INSPIRE].

[41] QCDSF-UKQCD collaboration, T. Bakeyev et al., *Nonperturbative renormalization and improvement of the local vector current for quenched and unquenched Wilson fermions*, *Phys. Lett.* **B 580** (2004) 197 [hep-lat/0305014] [INSPIRE].

[42] T. Bhattacharya, R. Gupta, W. Lee, S.R. Sharpe and J.M. Wu, *Improved bilinears in lattice QCD with non-degenerate quarks*, *Phys. Rev.* **D 73** (2006) 034504 [hep-lat/0511014] [INSPIRE].

[43] G. Martinelli, C. Pittori, C.T. Sachrajda, M. Testa and A. Vladikas, *A general method for nonperturbative renormalization of lattice operators*, *Nucl. Phys.* **B 445** (1995) 81 [hep-lat/9411010] [INSPIRE].

[44] V. Maillart and F. Niedermayer, *A specific lattice artefact in non-perturbative renormalization of operators*, arXiv:0807.0030 [INSPIRE].

[45] S. Borsányi et al., *QCD thermodynamics with dynamical overlap fermions*, *Phys. Lett.* **B 713** (2012) 342 [arXiv:1204.4089] [INSPIRE].

[46] G.I. Egri et al., *Lattice QCD as a video game*, *Comput. Phys. Commun.* **177** (2007) 631 [hep-lat/0611022] [INSPIRE].

JHEP08(2012)126